Pb-free ferroelectrics investigated with density functional theory: SnAl_{1/2}Nb_{1/2}O_{3} perovskites

Joseph W. Bennett, Ilya Grinberg, Peter K. Davies, and Andrew M. Rappe

Phys. Rev. B **83**, 144112 — Published 26 April 2011

DOI: 10.1103/PhysRevB.83.144112

Pb-free ferroelectrics investigated with density functional theory: $Sn(Al_{1/2}Nb_{1/2})O_3$ Perovskites

Joseph W. Bennett[a], Ilya Grinberg[a], Peter K. Davies[b] and Andrew M. Rappe[a,b]
(a) The Makineni Theoretical Laboratories, Department of Chemistry
(b) Department of Materials Science and Engineering
University of Pennsylvania, Philadelphia, PA 19104-6323
(Dated: February 14, 2011)

Interest in Pb-free ferroelectrics has intensified as the search for less toxic Pb replacements continues. Since Sn is isoelectronic with Pb, it has generated great interest. Most of this effort has focused on $SnTiO_3$. Even though it shows impressive ferroelectricity in calculations, synthesis has proved elusive. We therefore use density-functional theory (DFT) to investigate B-site alternatives that involve smaller size, to promote perovskite phase stability. In this paper, $Sn(Al_{1/2}Nb_{1/2})O_3$ (SAN) is investigated. We demonstrate that SAN is likely to be synthesizable, will be ferroelectric, and perhaps a good piezoelectric material as well. We discuss how cation displacements and their interactions affect the polarization of the solid solution. We also explore the electronic properties of the SAN solid solution and correlate them to the structural findings.

PACS numbers:

I. INTRODUCTION

The discovery of extremely high piezoelectric coefficients in $Pb(Mg_{1/3}Nb_{2/3})O_3$-$PbTiO_3$ (PMN-PT) relaxor ferroelectrics, and high transition temperatures in $BiScO_3$-$PbTiO_3$ solid solutions has inspired an intense effort to understand the properties of these materials as well as to explore the properties of new solid solutions[1–4]. One research strategy has been to investigate the replacement of the Pb atom on the perovskite A-site, motivated by the desire to replace the toxic Pb atoms with more benign species such as Bi, Ag and Sn.[5–7].

Substitution of Pb by Sn has only recently begun to be investigated. The Sn^{2+} cation contains a $5s^2$ stereochemically active lone electron pair, which should function in a similar fashion to the $6s^2$ of Pb and thus Sn could be a suitable replacement for Pb. A recently published theoretical examination of $SnTiO_3$, the Sn-analog of ferroelectric $PbTiO_3$ (PT), showed significant Sn off-centering along c, increasing both the c/a ratio and $\vec{P}$ relative to PT[8]. The ferroelectric instability of $SnTiO_3$ was also reported[9], where a detailed examination of the phonon spectra showed that a tetragonal phase is preferred to a cubic phase. Another theoretical paper by Matar *et al.* showed similar results for $SnTiO_3$, though they divulged that attempts at conventional synthesis were not successful[7]. If instead a microwave-hydrothermal synthesis is employed, solid solutions of $(Ba_{1-x}Sn_x)TiO_3$ could be cleanly obtained up to x=0.2[10,11]. A-site substitution of Sn into $(Ba_{1-x}Ca_x)TiO_3$ solid solution has been shown to enhance the Curie transition temperature even for $< 10\%$ substitution of Sn.[12]

Perovskite stability is related to the ratio of the ionic size of the A- and B-sites, as expressed by the tolerance factor, t:

$$t = \frac{R_{A-O}}{R_{B-O}\sqrt{2}} \tag{1}$$

where R_{A-O} is the sum of A and O ionic radii and R_{B-O} is the sum of B and O ionic radii[13]. Formation of the perovskite phase is favored when t is near unity. Using periodic trends of the Shannon-Prewitt radii, we estimate that in a 12-fold coordinated environment, the ionic radius of Sn^{2+}, $r_{Sn^{2+}}$, should be about 10% less that of Pb^{2+} (1.49 Å), or 1.35 Å[14]. Even for t close to 1, perovskite stability can be hindered by the partial reduction of Sn to Sn^0 or disproportionation to Sn^0 and Sn^{4+} at elevated temperatures. Therefore, the search for suitable B-sites should focus on small cations that tend to prevent reduction of Sn at high temperatures.

Inspection of the Shannon radii shows that Al (r_{Al}=0.53 Å) has the smallest ionic radius for 6-fold coordination of the cations commonly found on the B-site in perovskites[14]. To ensure charge balance and the average +4 charge on the B-site, Nb (r_{Nb}=0.64 Å) can be paired with Al. Nb has been shown to off-center in single crystal $LiNbO_3$[15] and the solid solution $Pb(Mg_{1/3}Nb_{2/3})O_3$ (PMN)[16,17]. The resultant $Sn(Al_{1/2}Nb_{1/2})O_3$ (SAN) solid solution should be close to the previously mentioned perovskite stability range, therefore increasing the chances for successful synthesis.

In this work, we use first-principles DFT to study the properties of ground state structures of the SAN solid solution. We elucidate the nature of the local environment, relating cation displacements and octahedral tilting to polarization.

II. METHODOLOGY

In the present study, cell parameters (lattice constants and angles) are optimized using the ABINIT software package[18]. An in-house solid state DFT code, BH, employed in previous studies[19,20] is used to relax the ionic positions of all atoms. We use the local density approximation (LDA) of the exchange correlation functional and a $4\times4\times4$ Monkhorst-Pack sampling of the Brillouin zone[21] for all calculations, except for the Berry phase polarization calculations for which a $6\times6\times6$ grid was used[22]. In order to calculate the phonon frequencies of each supercell at Γ, as well as the piezoelectric coefficients (ϵ_{ij}), we used density functional perturbation theory[23] and strain linear response calculations[24], respectively. We found no imaginary phonon frequencies at Γ and conclude that all supercells are dynamically stable. All calculations are performed with a plane wave cutoff of 50 Ry and all atoms are represented by norm-conserving optimized[25] designed nonlocal[26] pseudopotentials, generated by the OPIUM code[27]. Each of the B-site arrangements of $Sn(Al_{1/2}Nb_{1/2})O_3$ (SAN) is studied in a $2\times2\times2$ forty-atom supercell to reproduce any of the common three-dimensional tilt systems[28–30] that could be found experimentally.

III. RESULTS AND DISCUSSION

We find that for all SAN supercells studied, the ground state structure is ferroelectric with polarization values varying from 0.58 C/m^2 to 0.77 C/m^2. The orientation of the polarization vector varies according to B-site cation arrangement. With regards to the lattice constants, SAN supercells resemble either tetragonal (supercells 1, 2, 6) or orthorhombic (supercells 3, 4, 5) structures. For the majority of supercells, the difference between the c and a lattice constants is small, in contrast to the large c/a values found for $SnTiO_3$. In supercells 1, 2 and 6, the ratio between the polar and the non-polar axes ranges from 1.01 to 1.03. Similar ratios between the axes are found for supercells 3, 4 and 5. However, each contains at least one angle $\neq 90°$, decreasing macroscopic supercell symmetry to either monoclinic (supercells 1-4, 6) or triclinic (supercell 5), regardless of cation arrangement. Asymmetric cation displacements decrease the symmetry of all supercells to $P1$ symmetry.

We use the same ten supercells as in the work of Qi *et al.*[31], since the tetragonal symmetry associated with most common ferroelectrics would yield these ten unique structures. We find however that only supercells 1 through 6 are unique, while 7 through 10 relax to 2, 3, 4 and 5 respectively. These six supercells can be viewed as sampling the local B-cation arrangement resulting from quenched disorder on the B-site[17,32]. This disorder arises when the solid soluton is rapidly cooled during typical solid state synthesis. At high temperature, the B-cations are disordered and migrate freely between the sites. Rapid cooling freezes in the high temperature B-site cation disorder.

Comparison of total energies shows that energy differences between the different B-cation arrangements in SAN are similar to the standard electrostatically driven B-cation energetics found in Ba- and Pb-based perovskites. The standard model[33–35] predicts the rock-salt Al/Nb ordering to be the lowest energy. This is the case for $Ba(Sc_{1/2}Nb_{1/2})O_3$ (BSN) and $Pb(Sc_{1/2}Nb_{1/2})O_3$ (PSN) and we find this to be true for SAN also. The range of total energy differences ($\approx$0.7 eV/40-atom cell) is similar to that found by DFT calculations for PSN, in between those for the Ba-based[35] and Bi-based materials[31]. However, according to the standard model, the planar stacking of the B-cations will be the highest energy B-cation arrangement, as is found for BSN and PSN materials. In SAN solid solution though, we find that the planar stacking of Al and Nb is only slightly higher in energy (supercell 2) than the rock-salt Al/Nb arrangement and is much lower in energy than a variety of other B-cation arrangements including the (011) ordering. These (011) B-cation arrangements are unfavorable and will most likely only rarely be present in SAN.

For all supercells, the minimum energy volume is $\approx$ 60 Å^3, corresponding to a=3.90 Å. This is essentially identical to the LDA minimum energy volume found previously for $SnTiO_3$, as expected since the average ionic radius of Al and Nb ions is slightly smaller than that of Ti. For supercell 3, lattice constant a is smaller but the large value of lattice constant c makes the overall volume equal to that of $PbTiO_3$ material.

In this case, there is a (011) type B-cation ordering with unfavorable Nb^{5+}-Nb^{5+} interactions. Even though the supercell elongates in the direction of the most Nb-Nb pairs in response to the cation repulsion, this cation ordering is still unfavorable. In supercells 4, 5 and 6, Nb^{5+}-Nb^{5+} pairs are along a Cartesian axis in which Al^{3+}-Nb^{5+} pairs, as well as Al^{3+}-Al^{3+} pairs are present. This serves to decrease the unfavorable ionic interactions observed in supercell 3 and c/a is therefore close to 1. Due to their lower energies, these supercells are are more representative of the SAN solid solution.

The triclinic structure of supercell 5 found by our calculations for SAN is reminiscent of the low-symmetry structures observed in PMN-PT, PZT and other solid solutions at the morphotropic phase boundary (MPB) compositions.[32,36] In those cases, the potential energy surface for the P vector rotation is flat, leading to a high electromechanical response. The proximity of c/a to unity and the similarity of the structure of supercell 5 to those of MPB materials suggest that pure SAN is close to the MPB and with slight doping an MPB wih good electromechanical properties should be formed.

To test our hypothesis, we examine the piezoelectric coefficients of SAN supercells. As a solid solution approaches an MPB, the piezoelectric coefficients, ϵ_{ij}, increase, indicating that as cations move and $\vec{P}$ changes, a change in strain will also occur. We compute all elements of the piezoelectric tensor for the six unique SAN supercells (reported in the Appendix). It should be noted that the elements resemble more closely those of a class m monoclinic system and not a tetragonal or orthorhombic system. For all supercells, the diagonal piezoelectric coefficients are larger than e_{33}=2.7 C/m^2 found for $SnTiO_3$ by Uratani *et al.*[8]. With the exception of supercells 1 and 4 the diagonal e_{ii} coefficients are also larger than the $PbTiO_3$ e_{33} coefficient. In particular for supercell 5, we find e_{ii}=11.3 C/m^2, quite close to the e_{33}=12.6 C/m^2 previously found for 50/50 PZT[37]. This high e_{ij} is related to the fact that supercell 5 exhibits a monoclinic (211) orientation of the polarization vector, as 50/50 PZT does. Examination of the off-diagonal elements of the e tensor shows that for most supercells they are comparable to the e_{31} and e_{15} coefficients of $PbTiO_3$ and $SnTiO_3$. However, high values of the e_{15} (10.5 C/m^2) and e_{31} (7.3 C/m^2) coefficients are found in supercell 1 and supercell 5, respectively. These large piezoelectric coefficients support the hypothesis that SAN is close to the MPB.

Our previously developed theory for predicting the location of the MPB in a solid solution[38] can be used to estimate the compositional proximity of SAN to an MPB. In Pb-based solid solutions with $PbTiO_3$ (PT), the PT content at the MPB ($x_{\rm PT}^{\rm MPB}$) is given by

$$x_{\rm PT}^{\rm MPB} = 1 - 1/(0.34 + 3.31R_{\rm B,avg} - 7.49D_{\rm B,avg}^0), \tag{2}$$

where $R_{\rm B,avg}$ is the average Shannon ionic radius for the B-site and $D_{\rm B,avg}^0$ is the average reference ionic displacement of the B-site.

Equation 2 shows how both the displacement and size of the B-cations can be used as a guide to estimate how close a solid solution is to an MPB, and therefore how much tetragonal additive is needed to cross the phase boundary. The reference ionic displacements were evaluated previously from the B-cation ionic displacements obtained by DFT calculations of solid solutions with high PT content. Similarity between Pb and Sn behavior suggests that Equation 2 will be valid for Sn-based ferroelectrics as well. Comparison of Al and Nb displacements in SAN suggests that the reference ionic displacement of Al is slightly smaller than that for Nb (0.17 Å). We therefore assign a $D_{\rm B}^0$=0.11 Å to Al. Substituting the ionic radii for Al (0.53 Å) and Nb (0.64 Å) and $D_{\rm B}^0$ values into Equation 2 we obtain $x_{\rm PT}^{\rm MPB}$=0.18. Thus, only a small amount of tetragonal dopant into SAN will be necessary to result in a preference for tetragonal phase. Since $SnTiO_3$ exhibits a higher c/a ratio than PT, it is likely that less than 18% doping of $SnTiO_3$ will necessary to create an MPB in an SAN-$SnTiO_3$ solid solution.

To further support the hypothesis that SAN is close to an MPB, we directly calculate the energy cost of $\vec{P}$ rotation, using rocksalt ordered supercell 1 as our example. Though the ground state of this configuration is monoclinic, $\vec{P}$ along (011), we also obtain a stable local energy minimum tetragonal (α=β=γ=90°) structure with a=7.768 and c=7.905 Å, c/a=1.02, and $\vec{P}$ along (001). The difference in total energy between the monoclinic ground state and the tetragonal structure, with the *same* B-cation ordering, is small, 0.213 eV/40-atom cell.

Examination of all supercells show that the ionic displacements from high-symmetry positions are similar to those found previously for Pb-based perovskites. The polarization is caused by the concerted movement of Sn, Al and Nb cations from the center of their oxygen cages. As expected, the displacements of Sn atoms are much larger than those for the B-cations. Similar to the heterovalent Pb-based perovskites[17], Sn displaces toward the underbonded O atoms with two Al neighbors, and away from the overbonded O atoms with two Nb neighbors. This can be seen from a comparison of the Sn-Al and Sn-Nb partial pair distribution functions (PDFs) in Figure 2 (obtained from Structure 3), where the Sn-Al peaks are located at significantly smaller distances than the Sn-Nb peak.

Comparison of the Sn-O partial PDFs with Pb-O and Bi-O partial PDFs from previous work[6,32] allows us to assign an ionic size for a 12-fold coordinated Sn^{2+} (Figure 3). While all three PDFs exhibit three sets of peaks, due to creation of strong, medium and weak A-O bonds by the A-cation displacements, the peaks for the strong Sn-O bonds are located at smaller distances (2.3 Å) than the strong Pb-O bonds (2.5 Å). The weak Sn-O bonds are also shorter that the weak Pb-O bonds, as shown in Figure 3. This indicates that the ionic size of 12-fold coordinated Sn is smaller than that of Pb ($r_{\rm Pb}$=1.49 Å), allowing the Sn to come closer to the O atoms. The ionic size of Sn is larger than that of Bi ($r_{\rm Bi}$=1.36 Å), as can be seen by comparison of shortest Sn-O distances (2.3 Å) to the distances for the strongest Bi-O bonds (2.1 Å). We therefore estimate the ionic size of Sn^{+2} to be around 1.4 Å in the 12-fold coordination of the perovskite A-site. This yields t=1.00 for SAN solid solution and t=0.99 for $SnTiO_3$.

Examination of the octahedral tilt magnitudes in SAN provides further support for our assignment of $r_{\rm Sn^{2+}}$=1.4 Å. We find that octahedral tilts of the O_6 cages are rather small, ranging from 0° to 4°. This is similar to the octahedral tilts found in the 50/50 MPB composition of PZT, where t=0.99[32]. The small tilts of O_6 cages found for SAN similarly indicate that the preferred A-O and B-O distances in SAN are closely matched, with t close to one.

Despite a slightly higher value of the tolerance factor, which usually favors tetragonality, the c/a ratios for SAN supercells are much smaller than the c/a=1.10 value found for $SnTiO_3$. This is due to the differences in the B-site

chemistry between the two materials. The average displacements of both the Nb (0.17 Å) and Al ions (0.11 Å) are smaller than the Ti off-centering in either $PbTiO_3$ (0.28 Å) or $SnTiO_3$ (0.33 Å). The small B-site off-centering diminishes the strain-polarization coupling and makes large tetragonality unfavorable[39]. The small Nb displacements are most likely due to the larger ionic size of the Nb ion. For Al, the lack of d-states makes the Al-O bonding ionic which favors small displacements.

Turning our attention towards the electronic structure of SAN, examination of the DFT-LDA band structures shows that the indirect SAN band gap ranges from 1.7 to 2.2 eV, slightly higher than the DFT-LDA calculated gap for $PbTiO_3$ (1.5 eV). As an example, the electronic band structure of supercell 1 is shown in Figure 5. These DFT-LDA band gaps are underestimated, in line with previously reported trends[40,41]. There are slight differences between the nature of the valence and conduction bands of SAN and $PbTiO_3$. In ferroelectric $PbTiO_3$, the valence band is composed mainly of hybridized O $2p$ and Pb $6s$ orbitals, and the conduction band is composed mainly of Ti $3d$[42]. In SAN, the valence bands are mainly Sn $5s$ and O $2p$ orbitals, similar to $PbTiO_3$; however, there is also a significant amount of both Nb $5s$ and Al $3s$ character also present. The conduction band is mainly of Nb $4d$ character, similar to the Ti $3d$ of $PbTiO_3$, yet there is a slight amount of Sn $5p$ mixed into the band that overlaps with empty Al $3p$ states. This mixing of states could potentially be of interest as a way to decrease the band gap further by substituting more covalently bonded A- and B-site cations into SAN.

IV. CONCLUSION

We have presented calculations of the ground state structure and polarization of the Pb-free ferroelectric solid solution $Sn(Al_{1/2}Nb_{1/2})O_3$ (SAN). This material has t=1.00, within the range of experimentally feasible perovskite solid oxides, though synthesis of SAN could potentially be hindered by the chemical reactivity of Sn. We show that the properties of the ground state supercells resemble those previously found in ferroelectrics in close proximity to a morphotropic phase boundary, such as PZT. We believe that a slight amount of tetragonal additive can stabilize a tetragonal phase, creating an MPB and will also lead to an increase in polarization. To further support the proximity of SAN to an MPB, we find that for the rocksalt ordered supercell 1, the barrier to rotation of polarization from (011) to (001) is low. We also predict that the electronic structure of SAN is similar to that of $PbTiO_3$. The possibility of creating an MPB in a solid solution of SAN and $SnTiO_3$ is thus favorable for the development of Sn-based piezoelectrics to replace Pb-based perovskites used in current technologies.

V. ACKNOWLEDGMENTS

JWB and AMR were supported by the DoE Office of Basic Science, under grant number DE-FG02-07ER46431. IG was supported by the Office of Naval Research, under grant number N00014-09-1-0157. PKD acknowledges support from the Office of Naval Research through contract N00014-09-1-0455. Computational support was provided by US DoD, by a DURIP grant and by the HPCMO. The authors would like to acknowledge K. M. Rabe and D. R. Hamann for helpful discussions pertaining to the calculation of piezoelectric tensors.

[1] R. E. Eitel, C. A. Randall, T. R. Shrout, P. W. Rehrig, W. Hackenberger, and S.-E. Park, Jpn. J. Appl. Phys. **40**, 5999 (2001).
[2] J. Iñiguez, D. Vanderbilt, and L. Bellaiche, Phys. Rev. B **67**, 224107 (2003).
[3] R. E. Eitel, S. J. Zhang, T. R. Shrout, C. A. Randall, and I. Levin, J. Appl. Phys. **96**, 2828 (2004).
[4] Y. Inaguma, A. Miyaguchi, M. Yoshida, T. Katsumata, Y. Shimojo, R. Wang, and T. Sekiya, J. Appl. Phys. **95**, 231 (2004).
[5] I. Grinberg and A. M. Rappe, Appl. Phys. Lett. **85**, 1760 (2004).
[6] I. Grinberg, M. R. Suchomel, W. Dmowski, S. E. Mason, H. Wu, P. K. Davies, and A. M. Rappe, Phys. Rev. Lett. **98**, 107601 (2007).
[7] S. F. Matar, I. Baraille, and M. A. Subramanian, Chem. Phys. **355**, 43 (2009).
[8] Y. Uratani, T. Shishidou, and T. Oguchi, Jap. J. Appl. Phys. **47**, 7735 (2008).
[9] A. I. Lebedev, I. A. Sluchinskaya, and I. H. Munro, Phys. Solid State **51**, 362 (2009).
[10] Y. Xie, T. Hashimoto, H. Kimura, and T. Sato, J. Mater. Sci. **44**, 4834 (2009).
[11] Y. Xie, S. Yin, T. Hashimoto, H. Kimura, and T. Sato, J. Mater. Sci. **45**, 725 (2010).
[12] S. Suzuki, T. Takeda, and A. Ando, J. Appl. Phys. **96**, 132903 (2010).
[13] V. M. Goldschmidt, Die Naturwissenschaften **21**, 477 (1926).
[14] R. D. Shannon, Acta. Cryst. **A32**, 751 (1976).
[15] M. Veithen and P. Ghosez, Phys. Rev. B **65**, 214302 (2002).
[16] L. Bellaiche and D. Vanderbilt, Phys. Rev. Lett. **83**, 1347 (1999).
[17] I. Grinberg and A. M. Rappe, Phys. Rev. B **70**, 220101 (2004).
[18] X. Gonze, J.-M. Beuken, R. Caracas, F. Detraux, M. Fuchs, G.-M. Rignanese, L. Sindic, M. Verstraete, G. Zerah, F. Jollet, et al., Comp. Mater. Sci. **25**, 478 (2002).
[19] J. W. Bennett, I. Grinberg, and A. M. Rappe, Phys. Rev. B **73**, 180102(R) (2006).
[20] J. W. Bennett, I. Grinberg, and A. M. Rappe, Chem. Mat. **20**, 5134 (2008).
[21] H. J. Monkhorst and J. D. Pack, Phys. Rev. B **13**, 5188 (1976).
[22] R. Resta, Rev. Mod. Phys. **66**, 899 (1994).
[23] X. Gonze and C. Lee, Phys. Rev. B **55**, 10355 (1997).
[24] D. R. Hamann, X. Wu, K. M. Rabe, and D. Vanderbilt, Phys. Rev. B **71**, 035117 (2005).
[25] A. M. Rappe, K. M. Rabe, E. Kaxiras, and J. D. Joannopoulos, Phys. Rev. B Rapid Comm. **41**, 1227 (1990).
[26] N. J. Ramer and A. M. Rappe, Phys. Rev. B **59**, 12471 (1999).
[27] http://opium.sourceforge.net.
[28] A. M. Glazer, Acta Cryst. **28**, 3384 (1972).
[29] P. M. Woodward, Acta Cryst. **B53**, 32 (1997).
[30] P. M. Woodward, Acta Cryst. **B53**, 44 (1997).
[31] T. Qi, I. Grinberg, and A. M. Rappe, Phys. Rev. B. **79**, 094114 (2009).
[32] I. Grinberg, V. R. Cooper, and A. M. Rappe, Phys. Rev. B **69**, 144118 (2004).
[33] L. Bellaiche and D. Vanderbilt, Phys. Rev. Lett. **81**, 1318 (1998).
[34] L. Bellaiche, J. Padilla, and D. Vanderbilt, Phys. Rev. B **59**, 1834 (1999).
[35] B. P. Burton and E. Cockayne, Phys. Rev. B Rapid Comm. **60**, 12542 (1999).
[36] B. Noheda, Current Opinion in Solid State and Materials Science **6**, 27 (2002).
[37] Z. Wu and H. Krakauer, Phys. Rev. B **68**, 014112 (2003).
[38] I. Grinberg, M. R. Suchomel, P. K. Davies, and A. M. Rappe, J. Appl. Phys. **98**, 094111 (2005).
[39] T. Qi, I. Grinberg, and A. M. Rappe, Phys. Rev. B. **82**, 134113 (2010).
[40] L. J. Sham and M. Schlüter, Phys. Rev. Lett. **51**, 1888 (1983).
[41] C. G. van de Walle and R. M. Martin, Phys. Rev. B **34**, 5621 (1986).
[42] R. E. Cohen, Nature **358**, 136 (1992).

Figures

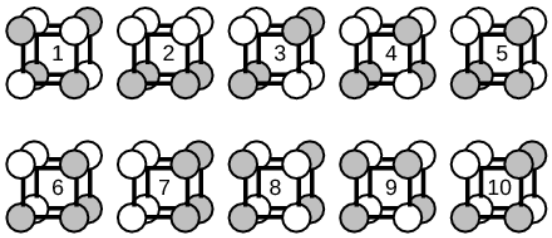

FIG. 1: B-site cation arrangements of $Sn(Al_{1/2}Nb_{1/2})O_3$ Supercells 1 through 10. Al is white and Nb is light gray.

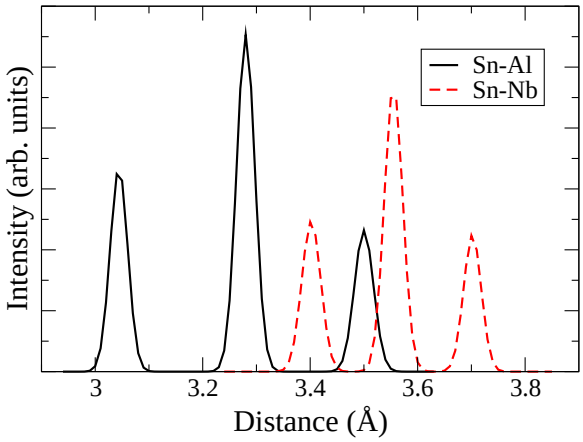

FIG. 2: Sn-Al and Sn-Nb partial PDFs shown as solid black and dashed red lines respectively. On average, Sn-Nb distances are larger than Sn-Al distances, demonstrating that Sn displacements are directed away from Nb and towards Al.

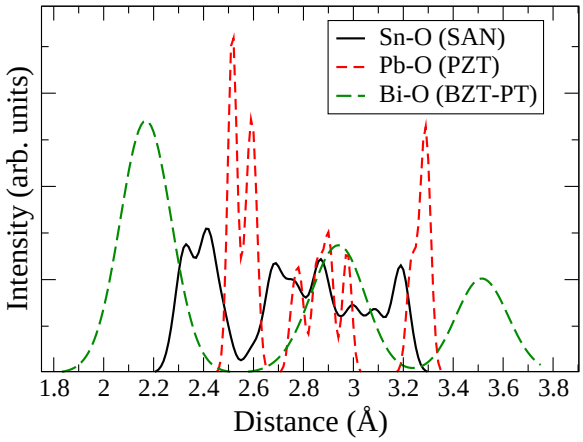

FIG. 3: Comparison of Sn-O, Pb-O and Bi-O partial PDFs. Sn-O shown in solid black line is obtained from current work. Pb-O and Bi-O data from previous work[6,32] are shown as dashed short (red) and long (green) lines respectively.

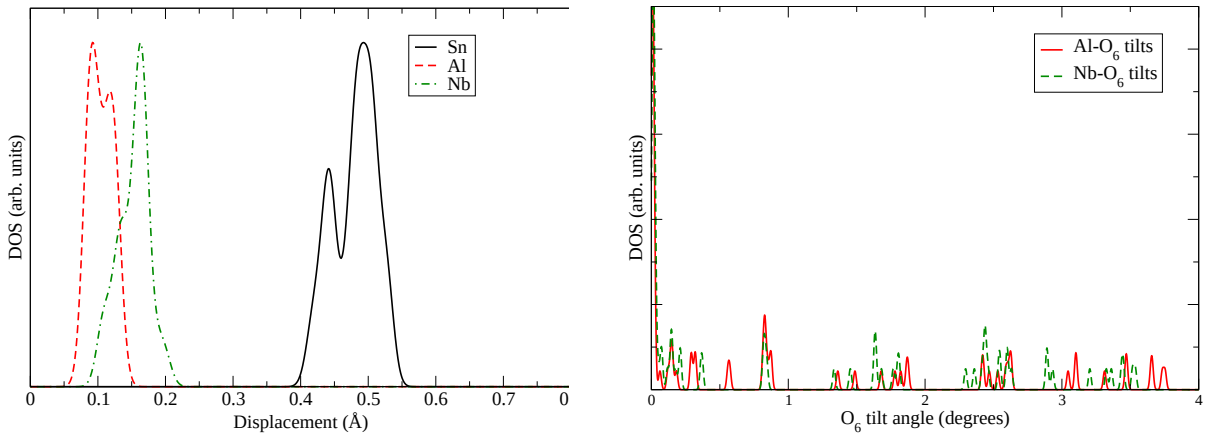

FIG. 4: The cation displacements and tilt angles are dependent on B-site cation arrangement. a) The displacement magnitudes for Sn (solid black), Al (dashed red) and Nb (dot-dashed green) vary; however on average Nb displaces further than Al. Sn displacement are larger than those of Al and Nb. b) The majority of octahedral tilts are well below 1° for both Al-O_6 (solid red) and Nb-O_6 (dashed green).

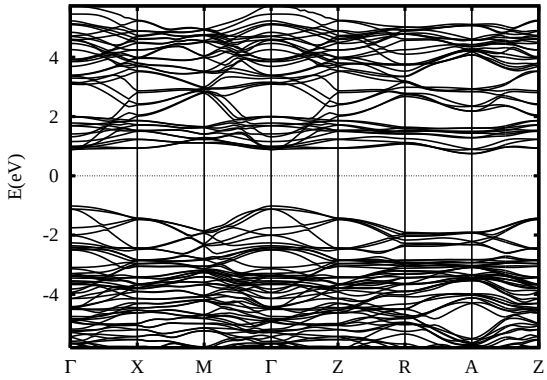

FIG. 5: DFT-LDA calculated electronic band structure of $SnAl_{1/2}Nb_{1/2}O_3$, supercell 1, with c/a=1.02. Indirect band gap (Γ to A) is 1.77 eV, slightly higher than previous calculations of $PbTiO_3$.

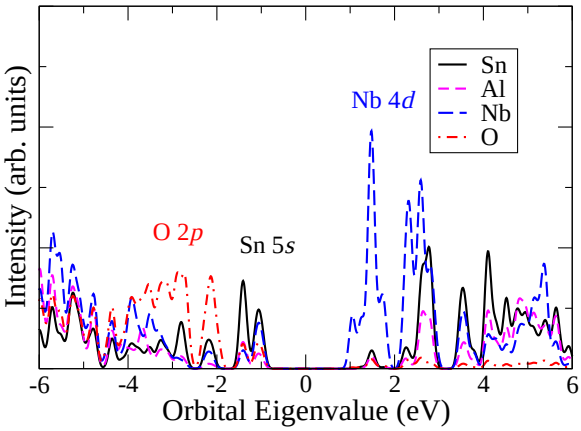

FIG. 6: Projected density of states of SAN supercell 1. The DFT-LDA calculated band gap is 1.77 eV. The valence band is composed mainly of Sn 5*s* orbital character, with Nb 4*d* character dominant in the conduction band.

Tables

Supercell	a	b	c	α	β	γ	P_x	P_y	P_z	$P_{\rm tot}$	$\rm E_{diff}$
1	7.789	7.887	7.887	89.5	90.0	90.0	0	0.43	0.43	0.61	0.000
2	7.938	7.933	7.777	90.0	90.0	89.5	0.54	0.54	0	0.77	0.039
3	7.806	8.033	7.825	89.3	90.0	90.0	0	0.52	0.34	0.62	0.699
4	7.831	7.942	7.858	89.5	90.00	90.00	0	0.46	0.41	0.62	0.408
5	7.887	7.874	7.868	90.1	90.2	89.7	0.44	0.28	0.25	0.58	0.406
6	7.917	7.784	7.918	90.0	90.5	90.0	0.53	0	0.52	0.74	0.067

TABLE I: Presented first are the supercell lattice constants in Å for $Sn(Al_{1/2}Nb_{1/2})O_3$ solid solution. Shown next are the angles between axes, the polarization in units of C/m^2 for all three directions, the total polarization and finally the difference in total energy relative to Supercell 1, in units of eV per 40-atom supercell.